ChemComm

COMMUNICATION

View Article Online
View Journal | View Issue

Cite this: *Chem. Commun.*, 2024, **60**, 2966

Received 3rd February 2024,
Accepted 15th February 2024

DOI: 10.1039/d4cc00546e

rsc.li/chemcomm

Temperature induced single-crystal to single-crystal transformation of uranium azide complexes†

Kai Li,[a] Thayalan Rajeshkumar,[b] Yue Zhao,[a] Tianwei Wang,[a] Laurent Maron *[b] and Congqing Zhu *[a]

The monomeric and dimeric uranium azide complexes {[(CH$_3$)$_2$NCH$_2$-CH$_2$NP^{i}Pr$_2$]$_2$U(N$_3$)$_2$} (2) and {[(CH$_3$)$_2$NCH$_2$CH$_2$NP^{i}Pr$_2$]$_2$U(N$_3$)$_2$}$_2$ (3) were synthesized by treating complex 1 with NaN$_3$ at 60 and −20 °C, respectively. A temperature-induced single-crystal to single-crystal transformation of 3 to 2 was observed. The reduction of either 2 or 3 with KC$_8$ yields a uranium nitride complex {[(CH$_3$)$_2$NCH$_2$CH$_2$-NP^{i}Pr$_2$]$_4$U$_2$(μ-N)$_2$} (4).

Single-crystal to single-crystal (SCSC) transformation is accompanied by the breaking of old chemical bonds and the formation of new bonds in the crystalline state, which can affect the dimensionality of complexes.[1] However, maintaining crystallinity during SCSC transformations is often challenging, which may contribute to their rarity and unpredictable nature.[2,3] Heating and light irradiation are two important external stimuli used to mediate SCSC transformations.[4,5] Whilst there are abundant examples of SCSC transformations reported for main group elements,[6] transition metals,[7] and rare-earth metals,[8] instances of such transformations for actinide elements are few.[9] Based on our ongoing interest in uranium chemistry supported by double layer N–P ligands,[10] we hereby report the isolation of monomeric and dimeric uranium azides **2** and **3** through salt metathesis between **1** and NaN$_3$ at different temperatures. A temperature-induced irreversible SCSC transformation from **3** to **2** was observed. In addition, the reactivity of **2** and **3** with KC$_8$ was investigated, leading to the isolation of uranium nitride **4**.

Treatment of complex **1** with two equivalents of NaN$_3$ in THF at room temperature (RT) for 10 h afforded a mixture containing both yellow crystalline complex **2** and green crystalline complex **3** after recrystallization at RT (Scheme 1). Interestingly, upon storing the filtrate of this reaction at 60 °C, we observed that the color of the filtrate changed from green to yellow, and the crystals of **2** were isolated with a 78% yield. Conversely, when the filtrate of this reaction was stored at −20 °C overnight, the crystals of **3** were formed with a 76% isolated yield (Scheme 1).

The structures of complexes **2** and **3** have been confirmed by single-crystal X-ray diffraction. Complex **2** is a monomer containing a single U center, which is coordinated by two monoanionic N–P ligands and two N_3^- units (Fig. 1). The bond lengths of U1–N1/N1′ (2.6990(18) Å) are longer than those of U1–N2/N2′ (2.2665(18) Å), reflecting the dative bond between U1 and N1/N1′. The bond lengths of U1–N3, N3–N4, and N4–N5 are 2.340(2) Å, 1.157(3) Å, and 1.152(3) Å, respectively. These bond lengths are consistent with the structure of U–N=N$^+$=N$^-$ for the terminal azide unit. The bond angles of U1–N3–N4 and N3–N4–N5 are 159.0(2)° and 179.7(3)°, respectively.

Complex **3** is a dimer containing two U centers connected by two N_3^- units (Fig. 2). The bond angles of U1–N8–N9 (140.0(10)°) and U1–N10–N11 (142.0(9)°) are smaller than the U1–N3–N4 angle (159.0(2)°) in complex **2**. The bond lengths of U1–N8 (2.546(11) Å) and U1–N10 (2.484(10) Å) are longer than the bond

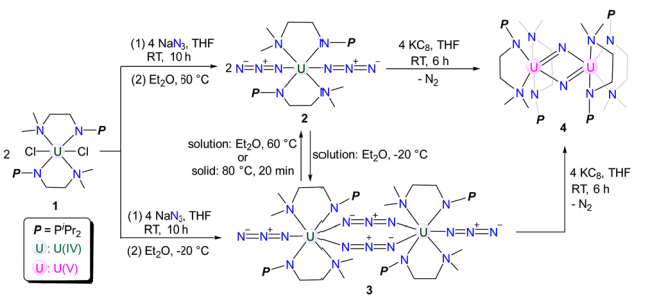

Scheme 1 Synthesis of complexes **2–4**.

[a] *State Key Laboratory of Coordination Chemistry, Jiangsu Key Laboratory of Advanced Organic Materials, School of Chemistry and Chemical Engineering, Nanjing University, Nanjing 210093, China. E-mail: zcq@nju.edu.cn*
[b] *LPCNO, CNRS & INSA, Université Paul Sabatier, 135 Avenue de Rangueil, Toulouse 31077, France. E-mail: laurent.maron@irsamc.ups-tlse.fr*

† Electronic supplementary information (ESI) available. CCDC 2310068–2310070 and 2329971–2329980. For ESI and crystallographic data in CIF or other electronic format see DOI: https://doi.org/10.1039/d4cc00546e

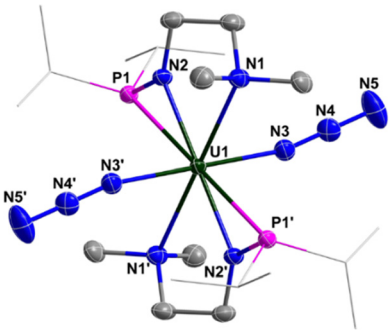

Fig. 1 Molecular structure of **2** with thermal ellipsoids at the 50% probability level. Hydrogen atoms are omitted for clarity. The ^{i}Pr groups on P atoms were simplified into lines.

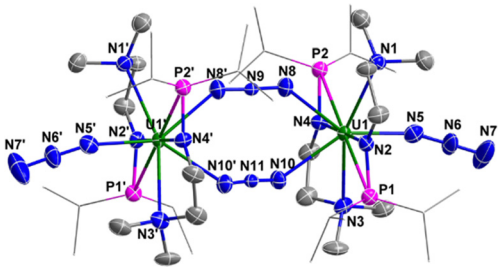

Fig. 2 Molecular structure of **3** with thermal ellipsoids at the 50% probability level. Hydrogen atoms are omitted for clarity. The ^{i}Pr groups on P atoms were simplified into lines.

length of U1–N5 (2.331(8) Å) due to the bridging nature of N8 and N10. Correspondingly, the bond lengths of N8–N9 (1.164(11) Å) and N10–N11 (1.180(10) Å) in the bridged N_3^- units are longer than those in the terminal N_3^- units, such as N6–N7 (1.151(14) Å).

In solution, complexes **2** and **3** can be interconverted at −20 °C and 60 °C. Consistently, the ^{1}H NMR spectra of complexes **2** or **3** recorded at RT demonstrated a 1 : 1 ratio between the monomer and dimer forms (Fig. S5 and S6, ESI†). Therefore, variable-temperature ^{1}H NMR spectra of complex **3** were measured in d_8-THF from 213 K to 333 K (Fig. 3). At 213 K, a range of signals between +82.1 and −76.3 ppm was attributed to resonances for complex **3**. As the temperature increased, the signals for complex **3** gradually disappeared, and a set of broad signals for complex **2** emerged, indicating the conversion from **3** to **2**. From these variable-temperature ^{1}H NMR spectral data, we calculated ΔH to be 3.2 ± 0.4 kcal mol^{-1} (Fig. S14, ESI†), which is in close proximity to the value obtained from DFT calculations (5.0 kcal mol^{-1}, Fig. S18, ESI†). Upon lowering the temperature from 333 K to 213 K, the signals for **2** disappeared and those for complex **3** reappeared (Fig. S1, ESI†). These results suggest that temperature-induced invertible transformation between complexes **2** and **3** is feasible in solution. The Fourier-transform infrared (FT-IR) spectra of complexes **2** and **3** were measured in the solid state at room temperature (Fig. S10 and S11, ESI†). Complex **3** exhibits two strong azide stretching vibrations at 2079 and 2134 cm^{-1}, characteristic of U-bound terminal and bridged azide ligands, whereas complex **2** shows a

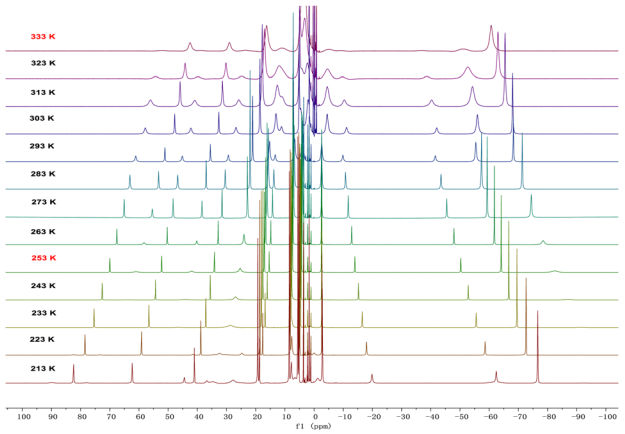

Fig. 3 Variable-temperature ^{1}H NMR spectra (from 213 K to 333 K) of complex **3** in d_8-THF.

single strong vibration at 2075 cm^{-1}, indicative of U-bound terminal azide ligands.[10a,11]

The UV-Vis-NIR electronic absorption spectra of complexes **2** and **3** were measured in THF at RT (Fig. S7, ESI†). Complexes **2** and **3** display an intense absorption peak at 227 nm and 238 nm, respectively. In addition, a weak absorption peak at 452 nm for complex **2** and at 456 nm for complex **3** is also observed in the visible region. Furthermore, a series of low-intensity absorptions are observed in the NIR region. For example, peaks at 821, 893, 1129, 1339, 1409, and 1510 nm were observed for complex **2**, while peaks at 819, 1129, 1335, 1427, and 1525 nm were observed for complex **3**. These low-intensity absorptions ($\varepsilon < 200$ M^{-1} cm^{-1}) in the NIR region for complexes **2** and **3** are attributed to the 5f–5f transitions, which are typical characteristics of U(IV) species.

Variable-temperature magnetic data for complexes **2** and **3** in the solid state were collected using a superconducting quantum interference device (SQUID) magnetometer (Fig. 4). The magnetic moment of complex **2** at 370 K is 3.10μ_B, which declines slowly to 2.49μ_B at 50 K, and then drops sharply to 0.55μ_B at 1.8 K with a trend toward zero. The effective moment for complex **3** at 1.8 K is 0.87μ_B, which increases sharply to 3.02μ_B at 50 K. With an increase in temperature from 50 K to 340 K, the magnetic moment of complex **3** reaches 3.31μ_B.

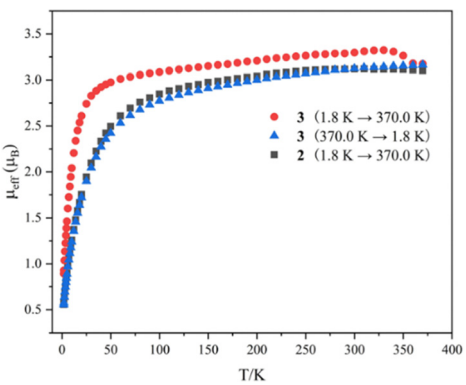

Fig. 4 Variable-temperature effective magnetic moment data. Magnetic moment per uranium ion for **2** and **3**.

When the temperature rises from 340 K to 370 K, the magnetic moments of complex **3** drop noticeably from 3.31 to 3.16μ_B, which is comparable to the moment of complex **2** at 370 K (3.10μ_B). With a reduction in temperature from 370 K to 1.8 K, the magnetic moment of complex **3** exhibits a similar trend and values to those of complex **2**. The magnitudes of μ_{eff} and the temperature dependence for complexes **2** and **3** are comparable to those observed for previously reported U(IV) complexes.[12] These results demonstrate that the dimeric complex **3** converts to the monomeric complex **2** at around 350 K in the solid state, suggesting a probable SCSC process.

To corroborate the process of SCSC transformation, two approaches were employed. Initially, a crystal of complex **3** was placed on a diffractometer and X-ray diffraction data were collected at different temperatures (313 K, 323 K, 333 K, 343 K, and 353 K). Analysis of these data revealed that complex **3** underwent a transformation to complex **2** at 353 K (Table S2, ESI†), which is further corroborated by a color change of the crystal from green to yellow at this temperature (Fig. S15, ESI†). The second method involved heating a crystal of complex **3** at incremental temperatures (40 °C, 50 °C, 60 °C, 70 °C, and 80 °C) within a glovebox for 20 minutes, followed by X-ray diffraction data collection at 193 K. The analysis of these data also confirmed that complex **3** converted to complex **2** after heating at 80 °C (Table S3, ESI†). Photographic evidence of the crystal additionally supports this transformation (Fig. S16, ESI†). The persistence of crystallinity during heating suggests an authentic SCSC transformation process.

Calculations were performed on **2** and **3** at the DFT level using the B3PW91 functional and including solvent effects (see ESI† for details). The formation of complex **2** from precursor **1** is exothermic by 16.5 kcal mol^{-1}. The dimerization of complex **2** to yield complex **3** is found to be exothermic by 5.0 kcal mol^{-1}, in line with the thermal equilibrium between complexes **2** and **3** reported experimentally. The optimized geometry is agreement with the experimental one, particularly the unsymmetrical coordination of the monoanionic N–P ligand (with U–N1 and U–N2 distances of 2.27 Å and 2.71 Å, respectively). Similarly, the azide coordination to the uranium is well reproduced, with the U–N3 distance being 2.35 Å. Natural Bonding Orbital (NBO) analysis indicates the presence of a polarized U–N3 bond (90% character on N) with a Wiberg Bond Index (WBI) of 0.78. The N3–N4 and N4–N5 WBIs are 1.71 and 2.14, respectively, consistent with the presence of two relatively covalent N=N double bonds interacting with a U(IV) center.

Geometry optimization was also performed on complex **3**, and different spin states were considered, namely the quintet, triplet, and open-shell singlet. The quintet and open-shell singlet states were found to be degenerate, while the triplet state is 10.5 kcal mol^{-1} higher in energy. The unpaired spin density plots (Fig. S20, ESI†) show that both uranium centers are in a +IV oxidation state. The distinction between the quintet and the open-shell singlet states lies in the spin coupling between the two U(IV) centers—ferromagnetic for the quintet and antiferromagnetic for the open-shell singlet—with the small energy difference indicating that there is no strong coupling between them. The associated UV-visible spectrum (Fig. S22, ESI†), computed in THF solution, displays intense absorption in the UV region with an absorption feature in the visible region (around 400 nm), corroborating the experimental observations.

Uranium azides are well-known precursors for the synthesis of uranium nitride *via* photolysis or reduction. However, the photolysis of complex **2** under a 40 W UV lamp for 10 hours only generates intractable results (Fig. S9, ESI†). Fortunately, treating complex **2** with two equivalents of KC_8 in THF affords a brownish solid, complex **4**, in a 67% yield after recrystallization from Et_2O at RT (Scheme 1). Complex **4** can also be synthesized by reducing complex **3** with four equivalents of KC_8 under the same conditions. The ^{1}H NMR spectrum of **4** exhibits five signals ranging from +7.6 to −30.1 ppm, with the signal of the N–CH_3 group located at −30.1 ppm.

The solid-state structure of complex **4** was determined by single-crystal X-ray diffraction (Fig. 5). The diamond-shaped U_2N_2 core is supported by four monoanionic N–P ligands. The U1–N9 (2.090(9) Å), U1–N10 (2.113(7) Å), U2–N9 (2.087(7) Å) and U2–N10 (2.068(8) Å) bond lengths are comparable to the U–N bond lengths in [{K(DME)(calix[4]tetrapyrrole)U^V}$_2$(μ-NK)$_2$][K(DME)$_4$] (2.076(6) and 2.099(5) Å),[13] [KU^V(μ-N)(OSi(O^{t}Bu)$_3$)$_3$]$_2$ (2.022(5) and 2.101(6) Å),[14] [Cs$_3${U^V(OSi(O^{t}Bu)$_3$)$_3$}(μ-N)$_2${U^V(OSi(O^{t}Bu)$_3$)$_2$-(κ-O)}][CsOSi(O^{t}Bu)$_3$] (1.85(1), 2.09(1), 2.13(1) and 2.34(1) Å),[15] [(μ-N)(U^V(N[^{t}Bu]Ar)$_3$)$_2$][B(Ar^F)$_4$] (Ar = 3,5-Me$_2$C$_6$H$_3$, Ar^F = 3,5-(CF$_3$)$_2$C$_6$H$_3$) (2.0470(3) and 2.0511(3) Å),[16] and in U(IV) nitride containing U_2N_2 core (2.153(2) Å).[17] However, these U–N bond lengths are slightly longer than terminal uranium(V) nitrides supported by Tren^{TIPS} ligand (1.80–1.89 Å).[18]

The UV-visible-NIR electronic absorption spectrum of complex **4** was measured in THF at room temperature (Fig. S12, ESI†), displaying an intense absorption peak at 225 nm and a series of low-intensity absorptions in the NIR region. These broad features in the NIR region are comparable to those reported for U(V) nitride.[11c,14,19] The effective magnetic moment at 300 K is 2.94μ_B (Fig. S13, ESI†), which is close to the theoretical value of 2.54μ_B for a U(V) ion.[10f,12] With decreasing temperature, the moment decreases to 0.83μ_B at 1.8 K per uranium. The variation in μ_{eff} and the temperature dependence

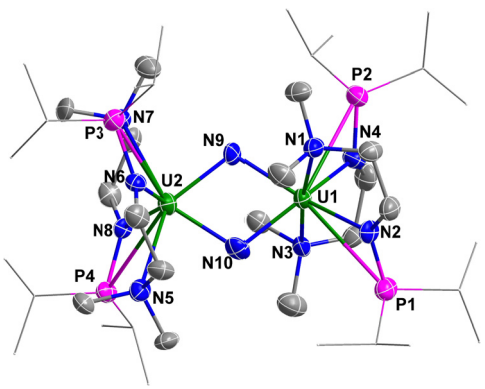

Fig. 5 Molecular structure of **4** with thermal ellipsoids at the 50% probability level. Hydrogen atoms are omitted for clarity. The ^{i}Pr groups on P atoms were simplified into lines.

of complex **4** are comparable to those of reported U(v) complexes.[20]

Finally, calculations on complex **4** considered three different spin states. The triplet and open-shell singlet were found to be degenerate, whereas the closed-shell singlet is higher in energy by 30.7 kcal mol^{-1}. The weak coupling between the two U centers is indicated by the small energy difference between the ferro- and antiferromagnetic states. The U═N Wiberg Bond Indices (WBIs) are 1.43 and 1.37, consistent with the presence of delocalized U═N double bonds. The U–U WBI is 0.5, highlighting electron delocalization within the U_2N_2 moiety.

In summary, monomeric and dimeric uranium azides, complexes **2** and **3**, were isolated by reacting complex **1** with NaN_3 at different temperatures. A temperature-induced irreversible SCSC transformation was observed from complex **3** to complex **2**. The uranium nitride complex **4**, featuring a U_2N_2 core, was isolated by reducing complexes **2** or **3** with KC_8.

This research was supported by the National Key R&D Program of China (2021YFA1502500), the National Natural Science Foundation of China (22271138), the Natural Science Foundation of Jiangsu Province (BK20220065). High Performance Computing Center of Nanjing University is also acknowledged. L. M. is a senior member of the Institut Universitaire de France. CalMip is acknowledged for a generous grant of computing time.

Conflicts of interest

The authors declare no competing financial interests.

Notes and references

1 (*a*) G. Chakraborty, I.-H. Park, R. Medishetty and J. J. Vittal, *Chem. Rev.*, 2021, **121**, 3751; (*b*) H. Wang, W. Meng, J. Wu, J. Ding, H. Hou and Y. Fan, *Coord. Chem. Rev.*, 2016, **307**, 130; (*c*) S. Kitagawa and K. Uemura, *Chem. Soc. Rev.*, 2005, **34**, 109; (*d*) Y. Chen, Q. Chen and Z. Zhang, *Chin. J. Org. Chem.*, 2021, **41**, 3826.

2 (*a*) J. J. Vittal, *Coord. Chem. Rev.*, 2007, **251**, 1781; (*b*) O. V. Zenkina, E. C. Keske, R. Wang and C. M. Crudden, *Angew. Chem., Int. Ed.*, 2011, **50**, 8100; (*c*) S. Rodríguez-Jiménez, H. L. C. Feltham and S. Brooker, *Angew. Chem., Int. Ed.*, 2016, **55**, 15067.

3 (*a*) C. G. Bezzu, M. Helliwell, J. E. Warren, D. R. Allan and N. B. Mckeown, *Science*, 2010, **327**, 1627; (*b*) M. Kawano and M. Fujita, *Coord. Chem. Rev.*, 2007, **251**, 2592; (*c*) Q. Liu, M. Lu, L. Yu, Y. Song and J. Lang, *Chin. J. Chem.*, 2021, **39**, 647; (*d*) Y. Cui and D. Xia, *Chin. J. Org. Chem.*, 2021, **41**, 907.

4 (*a*) G. K. Kole and J. J. Vittal, *Chem. Soc. Rev.*, 2013, **42**, 1755; (*b*) E. Fernandez-Bartolome, A. Martinez-Martinez, E. Resines-Urien, L. Pineiro-Lopez and J. S. Costa, *Coord. Chem. Rev.*, 2022, **452**, 214281; (*c*) W. He, S. Li and Y. Lan, *Inorg. Chem. Front.*, 2018, **5**, 279.

5 (*a*) S. Huang, T. Andy Hor and G. Jin, *Coord. Chem. Rev.*, 2017, **346**, 112; (*b*) B. B. Rath and J. J. Vittal, *Acc. Chem. Res.*, 2022, **55**, 1445; (*c*) Akhtaruzzaman, S. Khan, B. Dutta, T. S. Kannan, G. K. Kole and M. H. Mir, *Coord. Chem. Rev.*, 2023, **483**, 215095; (*d*) M. Zhang, X. Yang, Z. Xu, J. Yin and S. Liu, *Chin. J. Chem.*, 2022, **40**, 2853.

6 (*a*) A. J. Thompson, A. I. C. Orué, A. J. Nair, J. R. Piece, J. McMurtrie and J. K. Clegg, *Chem. Soc. Rev.*, 2021, **50**, 11725; (*b*) A. K. Saini, K. Natarajan and S. M. Mobin, *Chem. Commun.*, 2017, **53**, 9870.

7 (*a*) H. Li, S. Zhao, S. Zang and J. Li, *Chem. Soc. Rev.*, 2020, **49**, 6364; (*b*) E. A. Patrick, M. E. Bowden, J. D. Erickson, R. M. Bullock and B. L. Tran, *Angew. Chem., Int. Ed.*, 2023, e202304648.

8 (*a*) Y. So and W. Leung, *Coord. Chem. Rev.*, 2017, **340**, 172; (*b*) W. Chen, Y. Chen, G. Huang, J. Liu, J. Jia and M. Tong, *Chem. Commun.*, 2018, **54**, 10886; (*c*) Y. Xin, J. Wang, M. Zychowicz, J. J. Zakrzewski, K. Nakabayashi, B. Sieklucka, S. Chorazy and S.-I. Ohkoshi, *J. Am. Chem. Soc.*, 2019, **141**, 18211.

9 (*a*) K. Lv, S. Fichter, M. Gu, J. Marz and M. Schmidt, *Coord. Chem. Rev.*, 2021, **446**, 214011; (*b*) T. Zheng, Y. Gao, D. Gui, L. Chen, D. Sheng, J. Diwu, Z. Chai, T. Albrecht-Schmitt and S. Wang, *Dalton Trans.*, 2016, **45**, 9031; (*c*) Z. Xie, L. Mei, Q. Wu, K. Hu, L. Xia, Z. Chai and W. Shi, *Dalton Trans.*, 2017, **46**, 7392; (*d*) L. Chen, Y. Zhang, Z. Weng, Z. Liu, J. Zhang, Y. Wang and S. Wang, *Chin. J. Chem.*, 2021, **39**, 597; (*e*) L. Mei, L. Wang, L. Yuan, S. An, Y. Zhao, Z. Chai, P. C. Burns and W. Shi, *Chem. Commun.*, 2015, **51**, 11990.

10 (*a*) X. Xin, I. Douair, Y. Zhao, S. Wang, L. Maron and C. Zhu, *Natl. Sci. Rev.*, 2023, **10**, nwac144; (*b*) X. Xin, I. Douair, T. Rajeshkumar, Y. Zhao, S. Wang, L. Maron and C. Zhu, *Nat. Commun.*, 2022, **13**, 3809; (*c*) X. Xin, I. Douair, Y. Zhao, S. Wang, L. Maron and C. Zhu, *J. Am. Chem. Soc.*, 2020, **142**, 15004; (*d*) P. Wang, Y. Zhao and C. Zhu, *Organometallics*, 2022, **41**, 2448; (*e*) P. Wang, I. Douair, Y. Zhao, S. Wang, J. Zhu, L. Maron and C. Zhu, *Angew. Chem., Int. Ed.*, 2021, **60**, 473; (*f*) J. Shen, T. Rajeshkumar, G. Feng, Y. Zhao, S. Wang, L. Maron and C. Zhu, *Angew. Chem., Int. Ed.*, 2023, **62**, e202303379; (*g*) G. Feng, M. Zhang, D. Shao, X. Wang, S. Wang, L. Maron and C. Zhu, *Nat. Chem.*, 2019, **11**, 248; (*h*) G. Feng, M. Zhang, P. Wang, S. Wang, L. Maron and C. Zhu, *Proc. Natl. Acad. Sci. U. S. A.*, 2019, **116**, 17654; (*i*) P. Wang, I. Douair, Y. Zhao, R. Ge, J. Wang, S. Wang, L. Maron and C. Zhu, *Chemistry*, 2022, **8**, 1361; (*j*) G. Feng, K. N. McCabe, S. Wang, L. Maron and C. Zhu, *Chem. Sci.*, 2020, **11**, 7585; (*k*) W. Fang, S. Pan, W. Su, S. Wang, L. Zhao, G. Frenking and C. Zhu, *CCS Chem.*, 2022, **4**, 1921; (*l*) Q. Zhu, W. Fang, L. Maron and C. Zhu, *Acc. Chem. Res.*, 2022, **55**, 1718; (*m*) W. Fang, Q. Zhu and C. Zhu, *Chem. Soc. Rev.*, 2022, **51**, 8434; (*n*) X. Sun, X. Gong, Z. Xie and C. Zhu, *Chin. J. Chem.*, 2022, **40**, 2047; (*o*) W. Fang, I. Douair, A. Hauser, K. Li, Y. Zhao, P. W. Roesky, S. Wang, L. Maron and C. Zhu, *CCS Chem.*, 2022, **4**, 2630; (*p*) K. Li, J. He, Y. Zhao and C. Zhu, *Inorg. Chem. Front.*, 2023, **10**, 5622.

11 (*a*) R. K. Thomson, T. Cantat, B. L. Scott, D. E. Morris, E. R. Batista and J. L. Kiplinger, *Nat. Chem.*, 2010, **2**, 723; (*b*) R. Haiges, M. Vasiliu, D. A. Dixon and K. O. Christe, *Chem. – Eur. J.*, 2017, **23**, 652; (*c*) J. Du, D. M. King, L. Chatelain, E. Lu, F. Tuna, E. J. L. Mclnnes, A. J. Wooles, L. Maron and S. T. Liddle, *Chem. Sci.*, 2019, **10**, 3738.

12 D. R. Kindra and W. J. Evans, *Chem. Rev.*, 2014, **114**, 8865.

13 I. Korobkov, S. Gambarotta and G. Yap, *Angew. Chem., Int. Ed.*, 2002, **41**, 3433.

14 (*a*) C. Camp, J. Pécaut and M. Mazzanti, *J. Am. Chem. Soc.*, 2013, **135**, 12101; (*b*) L. Barluzzi, L. Chatelain, F. Fadaei-Tirani, I. Zivkovic and M. Mazzanti, *Chem. Sci.*, 2019, **10**, 3543; (*c*) L. Barluzzi, F.-C. Hsueh, R. Scopelliti, B. E. Atkinson, N. Kaltsoyannis and M. Mazzanti, *Chem. Sci.*, 2021, **12**, 8096.

15 N. Jori, T. Rajeshkumar, R. Scopelliti, I. Zivkovic, A. Sienkiewicz, L. Maron and M. Mazzanti, *Chem. Sci.*, 2022, **13**, 9232.

16 A. R. Fox, P. L. Arnold and C. C. Cummins, *J. Am. Chem. Soc.*, 2010, **132**, 3250.

17 D. M. King, B. E. Atkinson, L. Chatelain, M. Gregson, J. A. Seed, A. J. Wooles, N. Kaltsoyannis and S. T. Liddle, *Dalton Trans.*, 2022, **51**, 8855.

18 (*a*) D. M. King, F. Tuna, E. J. L. Mclnnes, J. McMaster, W. Lewis, A. J. Blake and S. T. Liddle, *Nat. Chem.*, 2013, **5**, 482; (*b*) D. M. King, P. A. Cleaves, A. J. Wooles, B. M. Gardner, N. F. Chilton, F. Tuna, W. Lewis, E. J. L. Mclnnes and S. T. Liddle, *Nat. Commun.*, 2016, **7**, 13773.

19 P. A. Cleaves, D. M. King, C. E. Kefalidis, L. Maron, F. Tuna, E. J. L. McInnes, J. McMaster, W. Lewis, A. J. Blake and S. T. Liddle, *Angew. Chem., Int. Ed.*, 2014, **53**, 10412.

20 (*a*) P. L. Arnold, A.-F. Pecharman, E. Hollis, A. Yahia, L. Maron, S. Parsons and J. B. Love, *Nat. Chem.*, 2010, **2**, 1056; (*b*) O. P. Lam, F. W. Heinemann and K. Meyer, *C. R. Chim.*, 2010, **13**, 803; (*c*) D. Patel, F. Moro, J. McMaster, W. Lewis, A. J. Blake and S. T. Liddle, *Angew. Chem., Int. Ed.*, 2011, **50**, 10388; (*d*) O. P. Lam, F. W. Heinemann and K. Meyer, *Chem. Sci.*, 2011, **2**, 1538; (*e*) D. M. King, F. Tuna, E. J. L. Mclnnes, J. McMaster, W. Lewis, A. J. Blake and S. T. Liddle, *Science*, 2012, **337**, 717; (*f*) D. Patel, F. Tuna, E. J. L. Mclnnes, J. McMaster, W. Lewis, A. J. Blake and S. T. Liddle, *Dalton Trans.*, 2013, **42**, 5224; (*g*) C. T. Palumbo, L. Barluzzi, R. Scopelliti, I. Zivkovic, A. Fabrizio, C. Corminboeuf and M. Mazzanti, *Chem. Sci.*, 2019, **10**, 8840.